Estimating the Ice Crystal Enhancement Factor in the Tropics

XIPING ZENG,*,+ WEI-KUO TAO,+ TOSHIHISA MATSUI,*,+ SHAOCHENG XIE,#
STEPHEN LANG,+,@ MINGHUA ZHANG,& DAVID O'C STARR,+ AND XIAOWEN LI*,+

* *Goddard Earth Sciences and Technology Center, University of Maryland, Baltimore County, Baltimore, Maryland*
\+ *Laboratory for Atmospheres, NASA Goddard Space Flight Center, Greenbelt, Maryland*
\# *Atmospheric Sciences Division, Lawrence Livermore National Laboratory, Livermore, California*
@ *Science Systems and Applications, Inc., Lanham, Maryland*
& *School of Marine and Atmospheric Sciences, Stony Brook University, Stony Brook, New York*

(Manuscript received 10 May 2010, in final form 28 January 2011)

ABSTRACT

The ice crystal enhancement (IE) factor, defined as the ratio of the ice crystal to ice nuclei (IN) number concentrations for any particular cloud condition, is needed to quantify the contribution of changes in IN to global warming. However, the ensemble characteristics of IE are still unclear. In this paper, a representation of the IE factor is incorporated into a three-ice-category microphysical scheme for use in long-term cloud-resolving model (CRM) simulations. Model results are compared with remote sensing observations, which suggest that, absent a physically based consideration of how IE comes about, the IE factor in tropical clouds is about 10^3 times larger than that in midlatitudinal ones. This significant difference in IE between the tropics and middle latitudes is consistent with the observation of stronger entrainment and detrainment in the tropics. In addition, the difference also suggests that cloud microphysical parameterizations depend on spatial resolution (or subgrid turbulence parameterizations within CRMs).

1. Introduction

Ice nuclei (IN), a class of aerosol particles, can significantly affect cloud ensembles via ice crystal concentration (Phillips et al. 2005, 2007; Ekman et al. 2007; Zeng et al. 2008), which in turn impacts radiation (e.g., Zeng et al. 2009b) and even global warming (e.g., Zeng et al. 2009a; DeMott et al. 2010). To quantify the effect of IN variability on global warming, it is imperative to know other dominant factors of ice crystal concentration besides IN. The ice crystal enhancement (IE) factor, defined as the ratio of the ice crystal concentration to the concentration of active IN in an air parcel, varies greatly from one cloud to another (Pruppacher and Klett 1997). Given its importance in modeling clouds and radiation (Zeng et al. 2008, 2009b), how to obtain its climatological characteristics (e.g., ensemble average, geographic distribution) is of great interest. In this paper, an assumed form of the IE factor is used in long-term cloud-resolving model (CRM) simulations and compared with field campaign remote sensing observations to infer general IE factor differences at different latitudes.

a. Ice crystal multiplication

Ice crystal multiplication processes are major contributors to the IE factor, but all of the mechanisms may not yet be understood. Ice crystal number concentrations often exceed IN concentrations estimated at the cloud-top temperature by up to four orders of magnitude [e.g., Koenig 1963; Mossop et al. 1968, 1970; Mossop 1985a; Hobbs and Rangno 1985, 1990; Blyth and Latham 1993; see Mossop (1985b) and Cooper (1986) for reviews]. A riming/splintering mechanism, identified by Hallett and Mossop (1974), is one candidate for high ice crystal multiplication (Blyth and Latham 1997; Phillips et al. 2001, 2007). This mechanism works when cloud temperatures are between −3° and −8°C and large droplets (≥24-μm diameter) as well as relatively fast falling (0.7 m s^{-1}) ice particles are present (e.g., Hallett and Mossop 1974; Mossop 1985a). Hence, it is of interest to parameterize ice crystal multiplication in a CRM, although absence of knowledge of all such processes will continue to limit this approach.

Corresponding author address: Dr. Xiping Zeng, C423, Bldg 33, Mail Code 613.1, NASA Goddard Space Flight Center, Greenbelt, MD 20771.
E-mail: xiping.zeng@nasa.gov

DOI: 10.1175/2011JAS3550.1

© 2011 American Meteorological Society

Blyth and Latham (1997), based on field observations, proposed a multithermal model of cloud glaciation and revealed that the riming/splintering mechanism contributes significantly to ice crystal multiplication via fine cloud dynamical structure. Using a three-dimensional (3D) high-resolution cloud model, Ovtchinnikov et al. (2000) explicitly simulated the fine dynamic structure and confirmed its importance in ice crystal multiplication.

Because of the effects of finescale cloud dynamics on microphysics, a CRM with a horizontal resolution of approximately 1 km must be reevaluated. Since the model cannot represent fine cloud dynamical structure explicitly, it cannot properly simulate the impacts of ice crystal multiplication. Thus, it is necessary to parameterize the ice crystal multiplication in a CRM via some assumed IE factor and then compare the modeled results with observations.

b. *Entrainment and detrainment in tropical clouds*

Fine cloud dynamical structure has been explored from aircraft observations (e.g., Malkus and Scorer 1955; Warner 1970; Paluch 1979; Blyth et al. 1988; Damiani et al. 2006). Updrafts usually take the form of entraining and detraining thermals, and the mixing between a thermal and its surrounding air takes place as a series of discrete events rather than continuously (e.g., Austin et al. 1985; Damiani et al. 2006). Since the mixed thermals eventually move to the level of zero buoyancy (Raymond and Blyth 1986; Taylor and Baker 1991; Emanuel 1994), mixing dominates the fine dynamical structure in clouds and therefore affects the vertical IE profile that results from ice multiplication processes.

However, the mixing varies greatly from one geographic region to another. Convective downdrafts, for example, which are quite common, have been observed to be more frequent in the tropics than in middle latitudes (e.g., Heymsfield et al. 1978; Wei et al. 1998; Igau et al. 1999). Zipser (2003), after reviewing the aircraft observations from over the past decades, concluded that undilute updraft cores have not been found in the tropics but are common in severe storms in middle latitudes. Based on this meridional variation in fine cloud dynamic structure, it is inferred that the IE factor in the tropics is much larger than that in middle latitudes (see section 4b for more discussion). This study aims to verify this variation by comparing CRM simulations that incorporate some assumed vertical IE profile with remote sensing cloud retrievals.

c. *Field observations and CRM simulations*

Recent CRM simulations have revealed that cloud ensembles and radiation are sensitive to the IE factor (e.g., Phillips et al. 2007; Zeng et al. 2008, 2009b). If a cloud simulation with an assumed IE factor can be made to match the associated observations, then the IE factor should be a better inference of the in situ one. This approach can be applied to estimate the IE factor over various geographic regions, with the aid of field campaign observations.

Three field campaigns have provided high-quality cloud observations as well as the corresponding large-scale forcing: the Tropical Warm Pool–International Cloud Experiment (TWP-ICE), the Kwajalein Experiment (KWAJEX), and the Atmospheric Radiation Measurement Program's spring 2000 cloud field campaign conducted around the Southern Great Plains site (ARM-SGP). Comparing the cloud observations from the three campaigns with CRM simulations, the IE factor over those regions can be estimated and further analyzed to determine how it varies meridionally.

The paper consists of five sections. In section 2, a CRM is described with special attention given to how to represent the IE factor and IN concentration. In section 3, CRM simulations are carried out and their results compared with observations to infer ice crystal concentrations. In section 4, three processes are reviewed connecting the IE factor and fine cloud dynamic structure, which are then used to explain the meridional variation in the IE factor. Section 5 provides the conclusions.

2. Experiment setup

A 3D CRM, the Goddard Cumulus Ensemble (GCE) model (Tao and Simpson 1993; Tao et al. 2003), is used to simulate clouds and radiation. The model is nonhydrostatic and anelastic. It takes account of both absorption and scattering for solar radiation and both emission and absorption for infrared radiation. Its cloud–radiation interaction has been assessed on a scale of 10^2 km (Tao et al. 1996). The model parameterizes subgrid-scale (turbulent) processes with a scheme based on Klemp and Wilhelmson (1978) and Soong and Ogura (1980) and incorporates the effects of both dry and moist processes on the generation of subgrid-scale kinetic energy. The model uses a three-category ice formulation based on Rutledge and Hobbs (1984) with some modifications (Lang et al. 2007; Zeng et al. 2008) for cloud microphysics. It includes the sedimentation of cloud ice (Starr and Cox 1985) to better simulate clouds in the upper troposphere. It calculates all scalar variables (temperature, water vapor, and all hydrometeors) with a positive definite advection scheme (Smolarkiewicz and Grabowski 1990). Modeled results [e.g., precipitable water, ice water content (IWC), radiative fluxes] have been compared with observations over the past decades to test the model's

performance (e.g., Johnson et al. 2002; Tao et al. 2003; Lang et al. 2007; Zeng et al. 2008, 2009b).

All of the numerical experiments in this study follow the model setup used in previous studies (e.g., Johnson et al. 2002; Xie et al. 2005; Xu et al. 2005; Blossey et al. 2007; Zeng et al. 2007), which simulated clouds with prescribed large-scale forcing derived from field observations. The experiments are 3D, using a 1-km horizontal resolution and a vertical resolution that ranges from 42.5 m at the bottom to 1 km at the top. The model uses $256 \times 256 \times 41$ grid points and a time step of 6 s for integration. Other model parameters are detailed in Zeng et al. (2008, 2009b).

The model has five prognostic hydrometeor variables: the mixing ratios of cloud water, rainwater, cloud ice, snow, and graupel. In brief, the model represents cloud microphysics with two water categories and three ice categories (referred to herein as a three-ice-category microphysical scheme).

Cloud ice and snow represent small and large crystals, respectively. They are segregated with an ice crystal 50 μm in diameter. In contrast to snow, graupel represents large crystals that are densely rimed. Thus, the present microphysics scheme uses a larger density for graupel (or 0.4 g cm^{-3}) but a smaller one for snow (or 0.1 g cm^{-3}). These categories of ice possess different terminal velocities and consequently stay aloft with different time scales.

The model represents the effects of the IE factor and IN concentration on the Bergeron process as follows. The conversion rate of cloud ice to snow due to vapor deposition is expressed as (Zeng et al. 2008, 2009b)

$$\max[2a_1(3q_i - m_{\mathrm{I50}}\rho^{-1}\mu N_i)m_{\mathrm{I50}}^{a_2-1}, 0],$$

and the conversion rate of cloud water to ice as

$$\frac{2}{(a_2+1)(a_2+2)}[3a_2q_i + (1-a_2)m_{\mathrm{I50}}\rho^{-1}\mu N_i]a_1m_{\mathrm{I50}}^{a_2-1},$$

where N_i is the number concentration of active ice nuclei, q_i the mixing ratio of cloud ice, a_1 and a_2 the temperature-dependent parameters in the Bergeron process (Koenig 1971), ρ the air density, and $m_{\mathrm{I50}} = 4.8 \times 10^{-7}$ g the mass of an ice crystal 50 μm in diameter; also, the parameter μ represents the IE factor due to riming/splintering and other mechanisms (Hallett and Mossop 1974; see section 4b for discussion).

Active IN concentration increases with decreasing air temperature (e.g., Fletcher 1962; Meyers et al. 1992; DeMott et al. 2010). Since there are no observations of IN and aerosol particles in the field campaigns, the model uses the simplest IN formula (Fletcher 1962) to compute the active IN concentration in the mixed-phase region as a function of air temperature T, or

$$N_i = n_0 \exp[\beta(T_0 - T)], \quad (1)$$

where n_0 and β are constant. To explore the effects of IN and IE on clouds and radiation, different IN concentrations and IE factors are tested for each large-scale forcing.

In this study, expression (1) represents the ensemble average of IN concentration over a sounding network that is approximately 100 km wide. Thus, the IN concentration cannot be compared directly with the aircraft observations at a specific location and time. Besides, the IN concentration and IE factor are combined into one factor in the present simulations. If a CRM simulation with specific values of μn_0 and β agrees well with field observations (i.e., radar, satellite, sounding networks and other measurements), then those values are treated as the in situ ones.

Table 1 shows the categories of ice crystal concentration used in the present simulations. When the ice crystal concentration is quite low (e.g., $\mu n_0 = 1.2 \times 10^{-9}$ cm^{-3} and $\beta = 0.4$), the present microphysical scheme degenerates into the default (or old) one.

TABLE 1. List of all the numerical simulations.

Field campaign	Numerical experiment	μn_0 (cm^{-3})	β	Ice crystal concentration
TWP-ICE	T06H	1.2×10^{-6}	0.6	High
	T06MH	1.2×10^{-7}	0.55	Moderately high
	T06M	1.2×10^{-8}	0.5	Moderate
	T06L	1.2×10^{-9}	0.4	Low
KWAJEX	K3DH	1.2×10^{-6}	0.6	High
	K3DL	1.2×10^{-9}	0.4	Low
ARM-SGP	A00H	1.2×10^{-6}	0.6	High
	A00M	1.2×10^{-8}	0.5	Moderate
	A00L	1.2×10^{-9}	0.4	Low

3. TWP-ICE simulations

In this section, CRM simulations over TWP-ICE are carried out and their results compared with remotely sensed cloud data to estimate the ice crystal concentration (or the product of IN concentration and the IE factor). Three simulations, T06L, T06M, and T06H, are carried out using low, moderate, and high ice crystal concentrations, respectively (see Table 1 for a summary; the terminology of low, moderate, and high is used for a brief description). Next, their results are compared with TWP-ICE observations to determine which category of crystal concentration brings about reasonable results.

TWP-ICE was conducted around Darwin, Australia, in January and February 2006 during the northern Australian

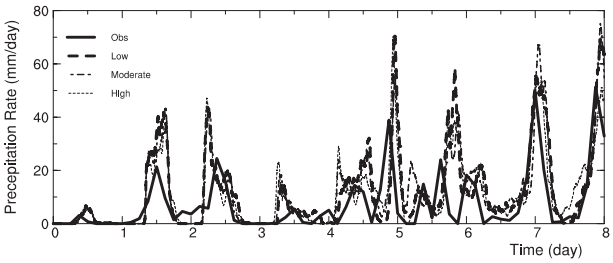

FIG. 1. Time series of surface precipitation rate for the TWP-ICE observations and three simulations that start at 2100 UTC 4 Feb 2006. The thick line represents the observations. Dashed, dotted–dashed, and dotted lines represent the modeling results with low (T06L), moderate (T06M), and high ice crystal concentrations (T06H), respectively.

monsoon (May et al. 2008). It was centered at 12°S, 131°E. It provided a great deal of information on clouds such as the liquid and ice water content retrieved from ARM Microbase products (Miller et al. 2003). It also provided large-scale forcing data (e.g., vertical motion and horizontal advective tendencies of temperature and moisture) derived using the variational analysis approach described in Zhang and Lin (1997) and Zhang et al. (2001). The large-scale forcing data represent the mean domain with a center at 12°S, 131°E and a radius of approximately 120 km [see Xie et al. (2010) for more details on the forcing]. The present study focuses on the period from 2100 UTC 4 February to 2100 UTC 12 February 2006, a typical monsoon break period, during which convection was characterized by intense afternoon thunderstorms with several squall lines crossing Darwin in the evening and early morning.

All three of the simulations start at 2100 UTC 4 February 2006 and last for 8 days. Figure 1 displays the 3-hourly average precipitation rate for the simulations. For comparison, it also displays an observed precipitation rate that is consistent with the large-scale forcing used. Generally speaking, the model captured the main precipitation events in spite of some quantitative deviations. The figure also shows that the ice crystal concentration can affect precipitation (e.g., days 1.5, 3.2, 4.5, 5.1, 5.8, 7, and 7.8).

Because both the large-scale forcing data and the model satisfy water balance in their frameworks, respectively, the effect of ice crystal concentration on precipitation is associated with that on precipitable water. As the ice crystal concentration increases from low to moderate to high, the modeled average precipitation rate decreases while the modeled average precipitable water amount increases from 49.4 to 51.4 mm. Compared to the observed precipitable water amount of 55.6 mm, a higher ice crystal concentration brings about more reasonable amount of precipitable water, which is consistent with previous results for the Global Atmospheric Research Program's (GARP's) Atlantic Tropical Experiment (GATE) simulations (Zeng et al. 2009b).

Moreover, ice crystal concentration can significantly affect cloud ensembles via the partitioning of ice species in the mixed-phase region. Figures 2 and 3 display time–pressure cross sections of the simulated ice contents using the low and high crystal concentrations, respectively. With increasing ice crystal concentration, the cloud ice content in the upper troposphere increases significantly. Correspondingly, snow increases while graupel decreases. This impact of ice crystal concentration on ice species is realized via supercooled droplets [see section 2.2 of Zeng et al. (2009a) for a complete discussion]. With increasing ice crystal concentration, the Wegener and Bergeron processes become stronger and consequently snow increases. Since snow competes with graupel at the expense of supercooled droplets in the upper mixed-phased region, graupel decreases there and falls into the lower mixed-phase region and then relatively weakens graupel riming there. As a result, more supercooled droplets survive, which results in an increase in cloud ice content in the upper troposphere.

The modeled ice content can be compared with the observed content to determine which category of crystal concentration, if any, is close to the in situ concentration. Figure 4 displays the vertical profile of the 8-day mean IWC retrieved from the radar observations over the Darwin station. The retrieval algorithm has been well tested on thin nonprecipitating clouds but not on thick precipitating clouds (Dong and Mace 2003). Figure 4 also displays the vertical profiles of mean modeled ice content (the sum of the cloud ice, snow, and graupel mixing ratios) for comparison; it shows that the IWC in the upper troposphere increases with increasing the ice crystal concentration in the mixed-phase region.

To better match the retrieved vertical profile in the upper troposphere, a new TWP-ICE simulation, T06MH, is carried out that uses a moderately high ice crystal concentration (or $\mu n_0 = 1.2 \times 10^{-7}$ cm^{-3} and $\beta = 0.55$). Figure 4 shows that the modeled ice profile from T06MH is close to the retrieved profile above 350 hPa.

However, all of the modeled ice contents differ greatly from the retrieved below the 350-hPa level. This difference between the retrieved and modeled contents is due not just to the model but also to the retrieval algorithm. In the retrieval algorithm, it is difficult to distinguish ice from liquid water using radar reflectivity, especially in the mixed-phase region (X. Dong 2008, personal communication). Hence, the retrieval in the mixed-phase region may contain a large error and therefore partly explains the difference between the retrieved and modeled ice contents below the 350-hPa level.

Observational sampling can also account for the difference between the retrieved and modeled IWCs below the

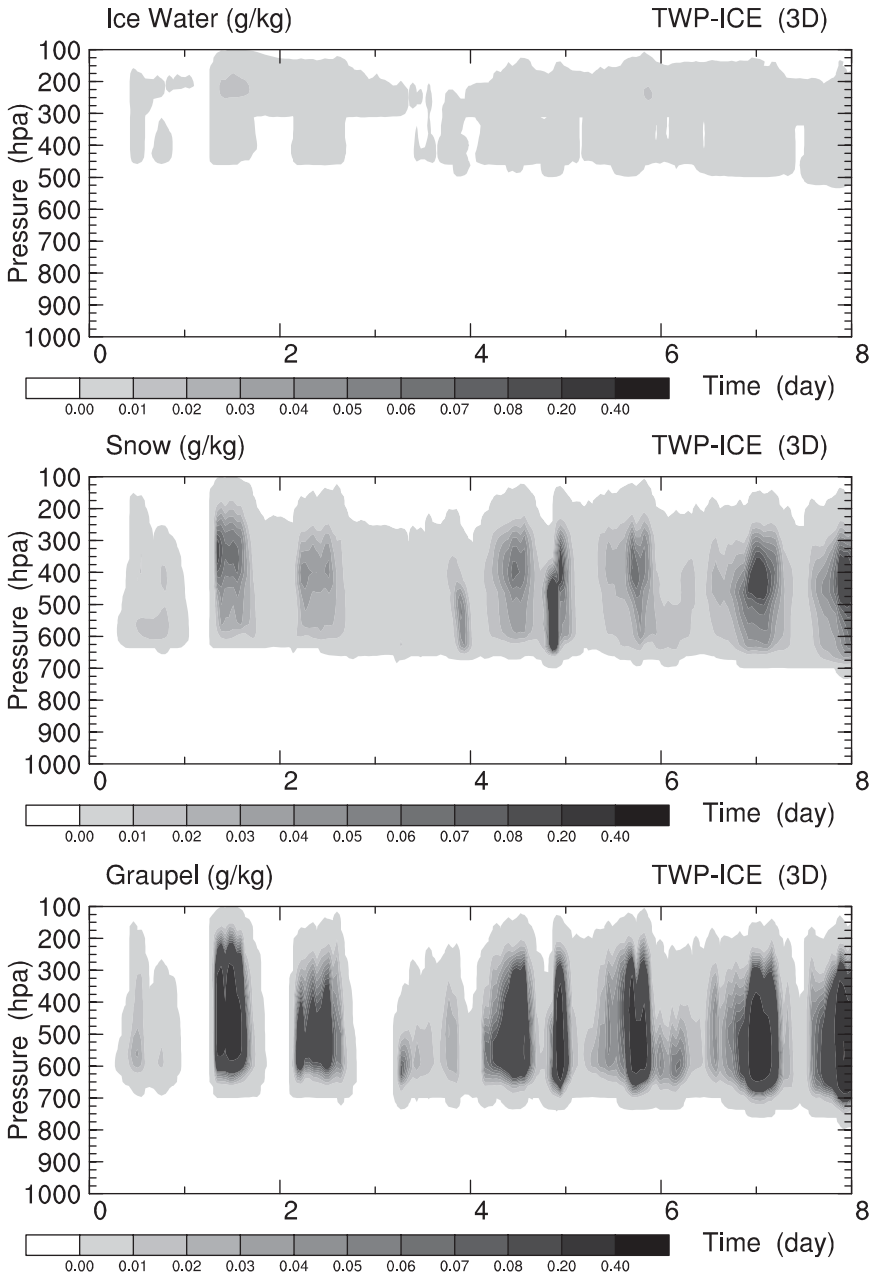

FIG. 2. Time–pressure cross sections of (top) cloud ice, (middle) snow, and (bottom) graupel mixing ratios for the TWP-ICE simulation T06L with the low ice crystal concentration.

350-hPa level. The modeled IWC in Fig. 4 represents the domain average of IWC. Thus, its peak at 500 hPa is attributed mainly to the graupel and snow in convective cores. In contrast, the observed IWC comes from the ARM radar that always points vertically and therefore cannot represent a domain average. Since convective cores cover only a small area, it is difficult for the radar to sample them sufficiently. Therefore, the radar may overlook the peak in IWC at 500 hPa. In contrast to convective cores, the cloud anvils that extend laterally outward from them cover a large area. Hence, the observed IWC can represent a domain average of IWC above 350 hPa.

Since ice particles, rather than supercooled drops, are common in the upper troposphere (e.g., above the 350-hPa level), the retrieval of IWC is reliable there (Dong and Mace 2003). Hence, based on the comparison between the modeled and retrieved IWCs above the 350-hPa level, it is inferred that the ice crystal concentration in the tropics is

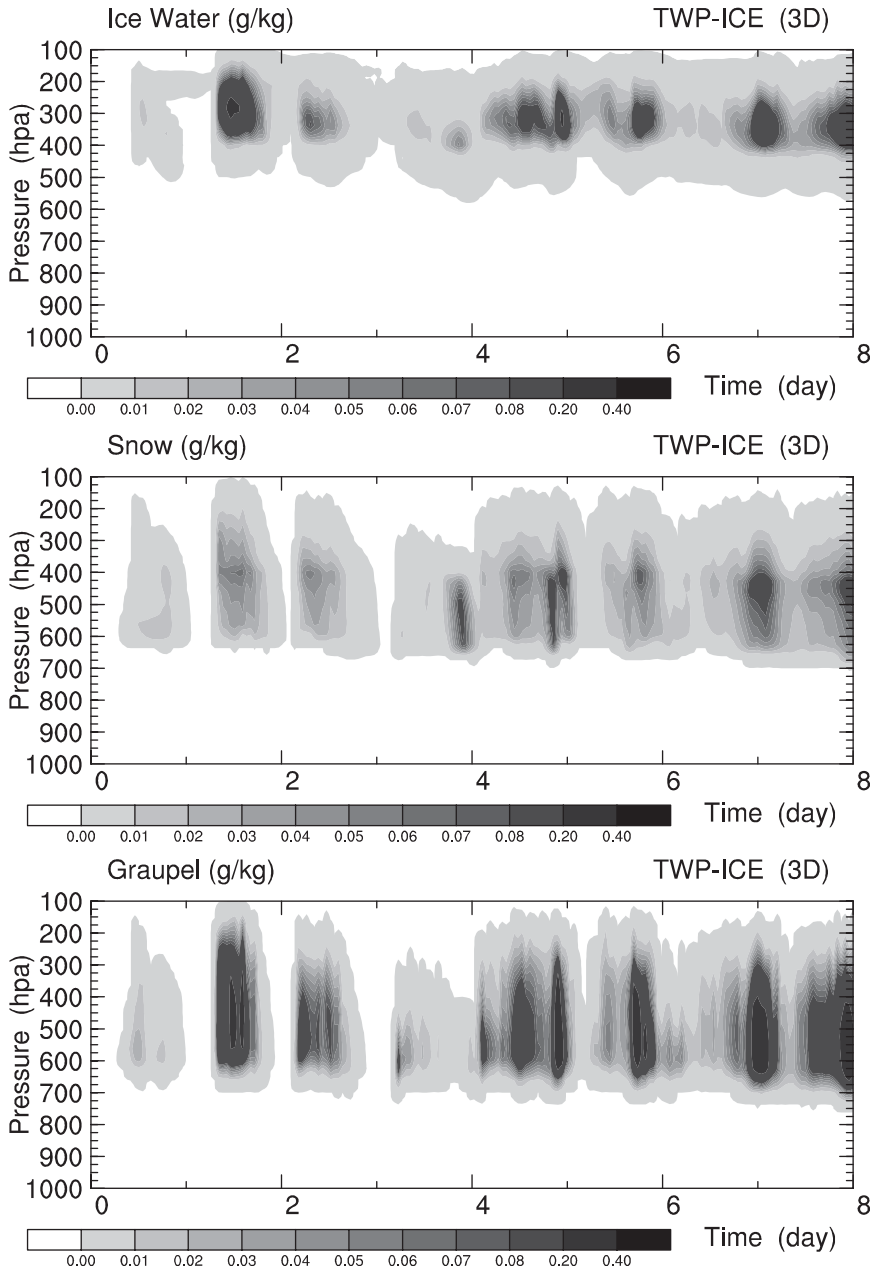

FIG. 3. As in Fig. 2, but for T06H with the high ice crystal concentration.

moderately high, which supports the preceding estimation of ice crystal concentration using observed precipitable water and precipitation rate.

4. Meridional variation in the IE factor

a. Comparing KWAJEX and ARM-SGP simulations with TWP-ICE

KWAJEX and ARM-SGP simulations using different ice crystal concentrations, which were carried out by Zeng et al. (2009a,b), are reviewed here in contrast to the TWP-ICE simulations to help infer the meridional variation of the IE factor. KWAJEX was centered at 8.8°N, 167.4°E. It took place over a tropical open ocean from 23 July through 15 September 1999. The two KWAJEX simulations start at 0600 UTC 24 July 1999 and last for 52 days. The simulations follow the same setup as those of TWP-ICE. The first simulation, K3DH, uses a high ice crystal concentration (or that of T06H), and the second one, K3DL, uses a low ice crystal concentration (or that of T06L). The modeled mean precipitation rate and precipitable water with the higher ice

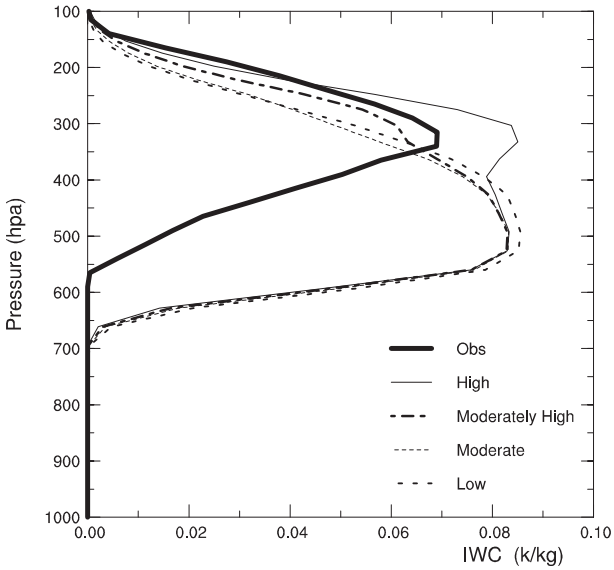

FIG. 4. Eight-day mean vertical profiles of IWC from the TWP-ICE observations (an ARM Microbase product; thick solid line) and the four simulations using the low (T06L; dashed line), moderate (T06M; dotted line), moderately high (T06MH; dotted–dashed line), and high ice crystal concentrations (T06H; thin solid line).

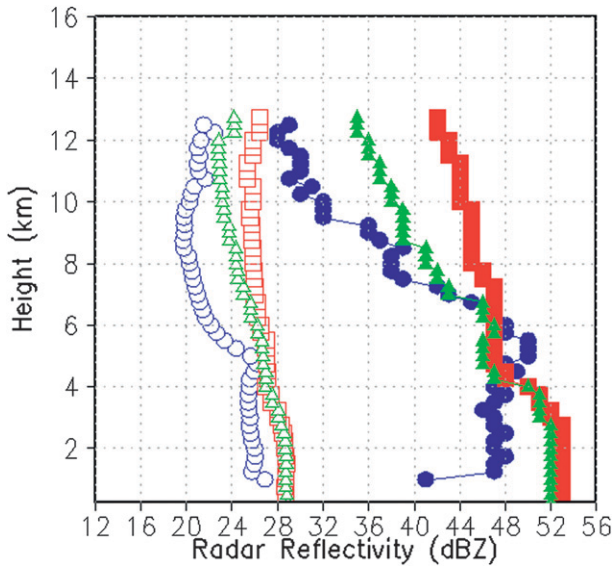

FIG. 5. Vertical distributions of radar reflectivity from KWAJEX observations and two simulations. Blue, red, and green symbols denote the observations and the simulations K3DL and K3DH with the low and high ice crystal concentrations, respectively. Open and solid symbols represent mean and maximum radar reflectivity, respectively.

crystal concentration are closer to the observed (Zeng et al. 2008).

The Precipitation Radar (PR) on the Tropical Rainfall Measuring Mission (TRMM) satellite (Simpson et al. 1988) flew over the KWAJEX region and thus provided vertical profiles of radar reflectivity during the campaign. Since the data are independent of the large-scale forcing data used, they provide further evidence regarding the sensitivity of the cloud ensembles to ice crystal concentration. Figure 5 displays vertical profiles of the mean and maximum radar reflectivity obtained from the TRMM observations over the period. The figure also displays the vertical profiles of simulated radar reflectivity sampled when the satellite flew over the campaign site [see Matsui et al. (2009) for the computational procedure]. As shown in the figure, the reflectivity profiles using the high crystal concentration are closer to the observed, especially in the upper troposphere, which supports the comparison in precipitable water and precipitation rate and the conclusion that the in situ ice crystal concentration is high.

Li et al. (2008) used a three-ice-category microphysical parameterization (similar to the present scheme with low ice crystal concentration or that of K3DL) to simulate a KWAJEX precipitation event on 11–12 August 1999 and found that the simulated radar reflectivities were 5–13 dBZ higher than those observed between 7 and 10.5 km where graupel is the dominant simulated ice species. The present two simulations cover this precipitation event. Their time–pressure cross sections of domain-averaged graupel mixing ratio and radar reflectivity from 0600 UTC 11 August to 0600 UTC 13 August 1999 (not shown) show that K3DH using the high ice crystal concentration reduces radar reflectivity and graupel significantly in the middle troposphere and subsequently is closer to the ground-based radar observations, which also supports the conclusion that the in situ ice crystal concentration is high.

The ARM-SGP simulations, in contrast to those from TWP-ICE and KWAJEX, lead to a different conclusion. Since the ARM-SGP campaign was centered at 36.6°N, 96.5°W and conducted during the spring of 2000, the simulations involved continental clouds in middle latitudes. Three ARM-SGP simulations with different ice crystal concentrations (A00H, A00M, and A00L; see Table 1 for details) were carried out, using the same setup as TWP-ICE and KWAJEX except that the surface fluxes were provided by observations. All of the simulations started at 1730 UTC 1 March 2000 and lasted for 20 days (Zeng et al. 2009a,b). Variables such as precipitable water, precipitation rate, and the infrared radiative flux at the top of the atmosphere change monotonically with ice crystal concentration and approach the observed when the ice crystal concentration is low. To further support the preceding estimation of in situ ice crystal concentration, radar observations are compared with cloud simulations. Figure 6, like Fig. 4, displays the vertical profile of IWC retrieved from radar observations. The figure also presents the vertical profiles of modeled IWC from the three

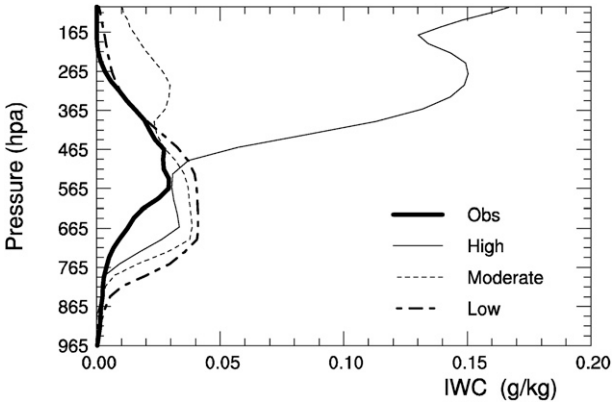

FIG. 6. Twenty-day mean vertical profiles of IWC from the ARM-SGP observations (thick solid line) and the three simulations using the low (A00L; dotted–dashed line), moderate (A00M; dashed line), and high ice crystal concentrations (A00H; thin solid line).

simulations. As shown in the figure, the IWC from the *low* ice crystal concentration is closer to the observed above the 400-hPa level, which indicates that the ice crystal concentration in spring is rather low in middle latitudes.

In brief, the TWP-ICE and KWAJEX simulations suggest that ice crystal concentrations in tropical clouds are high, but the ARM-SGP ones suggest that ice crystal concentrations in midlatitudinal clouds are low. This difference in ice crystal concentration is attributed to either a larger IN concentration or a larger IE factor in tropical clouds.

It is inferred that the ensemble averages of IN concentration in TWP-ICE and KWAJEX are not higher than those in ARM-SGP. The IN concentration is directly proportional to the aerosol concentration (e.g., DeMott et al. 2010), whose ensemble average in turn is proportional to aerosol production rate. Hence, the ensemble average of IN concentration is large over IN sources and small away from the sources. Since IN usually come from continents rather than oceans (e.g., Pruppacher and Klett 1997), it is inferred that the ensemble averages of IN concentration over TWP-ICE and KWAJEX are lower than those over ARM-SGP because TWP-ICE, KWAJEX, and ARM-SGP occurred respectively in coastal, oceanic, and continental regions. Suppose that the ensemble averages of IN concentration over TWP-ICE and KWAJEX are smaller than (or even equal to) those over ARM-SGP. The difference in crystal concentration category between the simulations with good results suggests that the IE factor over TWP-ICE and KWAJEX is 10^3 times larger than that over ARM-SGP at a temperature of $-10°C$.

b. *Connection of IE to convective downdrafts*

Three kinds of processes account for the large IE factor in the tropics: downward-moving parcels with prior heterogeneous ice nucleation, downward-moving parcels with prior homogeneous freezing (e.g., Phillips et al. 2007), and rime-splintering (e.g., Blyth and Latham 1997). They are discussed next to show their dependence on convective downdrafts or moist eddies.

1) HETEROGENEOUS ICE NUCLEATION

Heterogeneous ice nucleation increases the IE factor via moist eddies or mixing. Consider an air parcel that has a temperature lower than 0°C and a relative humidity of 100% with respect to water. The parcel fluctuates vertically around its original position because of moist turbulence. Let Δz_m denote the maximum vertical displacement of the parcel above its original position. The IE factor due to moist turbulence can be derived based on (1).

Suppose that the IN concentration exactly follows (1). Consider an air parcel that goes adiabatically upward from height z to $z + \Delta z_m$ first and then returns to its original position. As a result, the IE factor

$$\mu = \exp(\beta \gamma_s \Delta z_m), \tag{2}$$

where γ_s is the saturated adiabatic lapse rate. The preceding expression shows that the IE factor increases significantly with increasing Δz_m under the given Fletcher formula assumptions. Suppose $\beta = 0.6$ and $\gamma_s = 7°C\,km^{-1}$. Thus, $\mu = 10$ when $\Delta z_m = 548$ m, and μ reaches 10^3 when the vertical displacement is around 1.5 km. This ice crystal enhancement due to heterogeneous nucleation works effectively for air temperatures between 0° and −40°C, even though heterogeneous nucleation is not effective when the air temperature is between 0° and −10°C.

2) HOMOGENEOUS FREEZING

Homogeneous freezing increases the IE factor via convective downdrafts (Sassen and Dodd 1988; Heymsfield and Sabin 1989; Heymsfield and Miloshevich 1993; Heymsfield et al. 2005; Phillips et al. 2007). Consider an air parcel that rises above the −40°C level and then returns to its original position. Since all of the supercooled droplets freeze because of homogeneous nucleation at temperatures lower than −40°C, the IE factor becomes very large through prior homogeneous freezing. This ice crystal enhancement works efficiently right below the −40°C level. Phillips et al. (2007), using a cloud model with a double-moment bulk microphysics scheme, found that homogeneous freezing contributes significantly to ice crystal concentrations, although the mechanism is not fully represented in the present simulations.

3) ICE CRYSTAL MULTIPLICATION

Ice crystal multiplication can contribute to the IE factor greatly; this has already been modeled by Chisnell

and Latham (1976), Ovtchinnikov et al. (2000), Phillips et al. (2001, 2002, 2005), and others. Of all the known multiplication mechanisms, rime splintering is most efficient, although it requires a strict set of conditions (Hallett and Mossop 1974; Mossop 1985a). If an air parcel undergoes these conditions again and again via moist eddies, the ice crystal multiplication factor (or its resulting IE factor) can reach 10^3 (Blyth and Latham 1997). Phillips et al. (2007) analyzed cloud simulations and showed that this form of ice crystal multiplication is important in the lower part of the mixed-phase region.

All of the preceding processes contribute to the IE factor and its vertical profile via convective downdrafts or moist eddies. Thus, their effects depend on the occurrence of convective downdrafts. Fine cloud dynamical structure (e.g., convective downdrafts, mixing) has been explored from aircraft observations (e.g., Malkus and Scorer 1955; Warner 1970; Paluch 1979; Blyth et al. 1988; Damiani et al. 2006). Updrafts usually take the form of entraining and detraining thermals, and the mixing between a thermal and its surrounding air takes place as a series of discrete events rather than continuously (e.g., Austin et al. 1985; Damiani et al. 2006). Since the mixed thermals eventually move to the level of zero buoyancy (Raymond and Blyth 1986; Taylor and Baker 1991; Emanuel 1994), mixing dominates the fine dynamical structure in clouds and therefore affects ice crystal multiplication.

Convective updrafts and downdrafts determine the maximum vertical displacement of air parcels. Since the drafts vary in frequency from one geographic region to another, they can bring about a geographic variation in the IE factor. Aircraft observations show that there are a great many downdrafts in the tropics but not in middle latitudes (e.g., Warner 1970; Heymsfield et al. 1978; Wei et al. 1998; Igau et al. 1999). Also, undilute (or concentrated) updraft cores have not been found in the tropics but are common in severe storms in middle latitudes (Zipser 2003). Aircraft observations also show that ice crystal concentrations are quite small in updrafts cores but large along the edges and in downdrafts (e.g., Damiani et al. 2006). All of the observations are consistent with the concept that frequent downdrafts in the tropics contribute a great deal to the high ice crystal concentrations or large IE factor there.

5. Conclusions and discussion

Since both the IN concentration and IE factor strongly impact upper-tropospheric ice water content (e.g., Phillips et al. 2007; Zeng et al. 2008, 2009b), they are both important in quantifying the effect of IN variability on global warming (Zeng et al. 2009a; DeMott et al. 2010). Because of the sparse cloud sampling by aircraft, no ensemble information on the IE factor is currently available. In this paper, long-term cloud simulations are compared with field observations to infer a meridional variation in the IE factor, which is summarized as follows:

- Long-term CRM simulations are compared with TWP-ICE, KWAJEX, and ARM-SGP cloud observations. It is found that the IE factor (e.g., at a temperature of $-10°C$) in the tropics is approximately 10^3 times larger than that in middle latitudes.
- The significant decrease in the IE factor with increasing latitude makes physical sense. Fine cloud dynamic structure (e.g., convective downdrafts) can affect the IE factor greatly via *homogeneous/heterogeneous ice nucleation and ice crystal multiplication*. Since the fine dynamic structure varies significantly from one geographic region to another, the frequent downdrafts or strong vertical mixing in the tropics bring about the large IE factor there in combination with processes that apparently create copious numbers of ice crystals at temperatures as warm as $-20°C$.
- Consider CRMs with a horizontal resolution of approximately 1 km. Since they do not simulate moist eddies explicitly, they should parameterize the effect of moist eddies on ice crystal concentration. In the present study, CRM simulations with different assigned crystal concentrations are compared with observations to infer (or diagnose) in situ crystal concentrations. It is found that the ice crystal concentration or IE factor varies significantly with latitude. In other words, the prediction or representation of ice crystal concentration in a CRM should be coupled with the subgrid turbulence parameterization, which is usually overlooked in current CRMs.
- After the IE factor is introduced into the Rutledge–Hobbs scheme, the scheme can be used to model clouds not only in middle latitudes but also in the tropics and can therefore provide a prototype version for future global CRM simulations.

In this study, radar and satellite observations and CRM simulations are used to indirectly estimate the IE factor. Further studies are needed to quantify the difference in the IE factor between middle latitudes and the tropics because many factors have not been quantified in the present study, such as IN concentration and its variation with temperature, relative humidity, and aerosol properties (e.g., DeMott et al. 2003). Besides, high-resolution cloud simulations are also needed to address why convective downdrafts are more frequent in the tropics than in middle latitudes.

Acknowledgments. This research was supported by the Office of Science (BER), U.S. Department of

Energy/Atmospheric System Research (DOE/ASR) Interagency Agreement DE-AI02-04ER63755 and -09ER64753. It was also supported by the NASA MAP project under Grant NNX09AJ46G and the NASA and DOE Atmospheric System Research Programs at the Stony Brook University. Dr. Xie, working at LLNL, was supported under the auspices of the U. S. Department of Energy/Office of Science, Biological and Environmental Research by the University of California Lawrence Livermore National Laboratory under Contract DE-AC52-07NA27344. The authors greatly appreciate the anonymous reviewers for their critical yet constructive comments. The authors acknowledge the NASA Ames Research Center and the NASA Goddard Space Flight Center for the computer time used in this research.

This paper is dedicated to Dr. Joanne Simpson, who passed away on 4 March 2010. Dr. Simpson was the leader of the Goddard Mesoscale Dynamics and Modeling group from 1987 to 2004. She taught the authors (W.-K. Tao, S. Lang, X. Li, and X. Zeng) to appreciate the value of using observations to validate simulated cloud processes.

REFERENCES

Austin, P. H., M. B. Baker, A. M. Blyth, and J. B. Jensen, 1985: Small-scale variability in warm continental cumulus clouds. *J. Atmos. Sci.,* **42,** 1123–1138.

Blossey, P. N., C. S. Bretherton, J. Cetrone, and M. Kharoutdino, 2007: Cloud-resolving model simulations of KWAJEX: Model sensitivities and comparisons with satellite and radar observations. *J. Atmos. Sci.,* **64,** 1488–1508.

Blyth, A. M., and J. Latham, 1993: Influence of glaciation on an effective-radius parametrization. *Quart. J. Roy. Meteor. Soc.,* **119,** 1469–1474.

——, and ——, 1997: A multi-thermal model of cumulus glaciation via the Hallett–Mossop process. *Quart. J. Roy. Meteor. Soc.,* **123,** 1185–1198.

——, W. A. Cooper, and J. B. Jensen, 1988: A study of the source of entrained air in Montana cumuli. *J. Atmos. Sci.,* **45,** 3944–3964.

Chisnell, R. F., and J. Latham, 1976: Ice particle multiplication in cumulus clouds. *Quart. J. Roy. Meteor. Soc.,* **102,** 133–156.

Cooper, W. A., 1986: Ice initiation in natural clouds. *Precipitation Enhancement: A Scientific Challenge, Meteor. Monogr.,* No. 43, Amer. Meteor. Soc., 29–32.

Damiani, R., G. Vali, and S. Haimov, 2006: The structure of thermals in cumulus from airborne dual-Doppler radar observations. *J. Atmos. Sci.,* **63,** 1432–1450.

DeMott, P. J., D. J. Cziczo, A. J. Prenni, D. M. Murphy, S. M. Kreidenweis, D. S. Thomson, R. Borys, and D. C. Rogers, 2003: Measurements of the concentration and composition of nuclei for cirrus formation. *Proc. Natl. Acad. Sci. USA,* **100,** 14 655–14 660.

——, and Coauthors, 2010: Predicting global atmospheric ice nuclei distributions and their impacts on climate. *Proc. Natl. Acad. Sci. USA,* **107,** 11 217–11 222.

Dong, X., and G. G. Mace, 2003: Profiles of low-level stratus cloud microphysics deduced from ground-based measurements. *J. Atmos. Oceanic Technol.,* **20,** 42–53.

Ekman, A. M. L., A. Engstrom, and C. Wang, 2007: The effect of aerosol composition and concentration on the development and anvil properties of a continental deep convective cloud. *Quart. J. Roy. Meteor. Soc.,* **133,** 1439–1452.

Emanuel, K. A., 1994: *Atmospheric Convection*. Oxford University Press, 580 pp.

Fletcher, N. H., 1962: *The Physics of Rain Clouds*. Cambridge University Press, 386 pp.

Hallett, J., and S. C. Mossop, 1974: Production of secondary ice particles during the riming process. *Nature,* **249,** 26–28.

Heymsfield, A. J., and R. M. Sabin, 1989: Cirrus crystal nucleation by homogeneous freezing of solution droplets. *J. Atmos. Sci.,* **46,** 2252–2264.

——, and L. Miloshevich, 1993: Homogeneous ice nucleation and supercooled liquid water in orographic wave clouds. *J. Atmos. Sci.,* **50,** 2335–2353.

——, P. N. Johnson, and J. E. Dye, 1978: Observations of moist adiabatic ascent in northeast Colorado cumulus congestus clouds. *J. Atmos. Sci.,* **35,** 1689–1703.

——, L. M. Miloshevich, C. Schmitt, A. Bansemer, C. Twohy, M. R. Poellot, A. Fridlind, and H. Gerber, 2005: Homogeneous ice nucleation in subtropical and tropical convection and its influence on cirrus anvil microphysics. *J. Atmos. Sci.,* **62,** 41–64.

Hobbs, P. V., and A. L. Rangno, 1985: Ice particle concentrations in clouds. *J. Atmos. Sci.,* **42,** 2523–2549.

——, and ——, 1990: Rapid development of high ice particle concentrations in small polar maritime cumuliform clouds. *J. Atmos. Sci.,* **47,** 2710–2722.

Igau, R. C., M. A. LeMone, and D. Wei, 1999: Updraft and downdraft cores in TOGA COARE: Why so many buoyant downdraft cores? *J. Atmos. Sci.,* **56,** 2232–2245.

Johnson, D. E., W.-K. Tao, J. Simpson, and C.-H. Sui, 2002: A study of the response of deep tropical clouds to large-scale thermodynamic forcing. Part I: Modeling strategies and simulations of TOGA COARE convective systems. *J. Atmos. Sci.,* **59,** 3492–3518.

Klemp, J. B., and R. B. Wilhelmson, 1978: The simulation of three-dimensional convective storm dynamics. *J. Atmos. Sci.,* **35,** 1070–1096.

Koenig, L. R., 1963: The glaciating behavior of small cumulonimbus clouds. *J. Atmos. Sci.,* **20,** 29–47.

——, 1971: Numerical modeling of ice deposition. *J. Atmos. Sci.,* **28,** 226–237.

Lang, S., W.-K. Tao, R. Cifelli, W. Olson, J. Halverson, S. Rutledge, and J. Simpson, 2007: Improving simulations of convective systems from TRMM LBA: Easterly and westerly regimes. *J. Atmos. Sci.,* **64,** 1141–1164.

Li, P., E. J. Zipser, S. K. Krueger, and M. K. Zulauf, 2008: Cloud-resolving modeling of deep convection during KWAJEX. Part I: Comparison to TRMM satellite and ground-based radar observations. *Mon. Wea. Rev.,* **136,** 2699–2712.

Malkus, J. S., and R. S. Scorer, 1955: The erosion of cumulus towers. *J. Meteor.,* **12,** 43–57.

Matsui, T., X. Zeng, W.-K. Tao, H. Masunaga, W. S. Olson, and S. Lang, 2009: Evaluation of long-term cloud-resolving model simulations using satellite radiance observations and multi-frequency satellite simulators. *J. Atmos. Oceanic Technol.,* **26,** 1261–1274.

May, P. T., J. H. Mather, G. Vaughan, K. N. Bower, C. Jakob, G. M. McFarquhar, and G. G. Mace, 2008: The Tropical Warm Pool International Cloud Experiment. *Bull. Amer. Meteor. Soc.,* **89,** 629–645.

Meyers, M. P., P. J. DeMott, and W. R. Cotton, 1992: New primary ice-nucleation parameterizations in an explicit cloud model. *J. Appl. Meteor.,* **31,** 708–721.

Miller, M. A., K. L. Johnson, D. T. Troyan, E. E. Clothiaux, E. J. Mlawer, and G. G. Mace, 2003: ARM value-added cloud products: Description and status. *Proc. 13th ARM Science Team Meeting,* Broomfield, CO, U.S. Dept. of Energy. [Available online at http://www.arm.gov/publications/proceedings/conf13/extended_abs/miller-ma.pdf.]

Mossop, S. C., 1985a: Secondary ice particle production during rime growth: The effect of drop size distribution and rimer velocity. *Quart. J. Roy. Meteor. Soc.,* **111,** 1113–1124.

——, 1985b: The origin and concentration of ice crystals in clouds. *Bull. Amer. Meteor. Soc.,* **66,** 264–273.

——, R. E. Ruskin, and K. J. Heffernan, 1968: Glaciation of cumulus at approximately −4°C. *J. Atmos. Sci.,* **25,** 889–899.

——, A. Ono, and E. R. Wishart, 1970: Ice particle in maritime near Tasmania. *Quart. J. Roy. Meteor. Soc.,* **25,** 487–508.

Ovtchinnikov, M., Y. L. Kogan, and A. M. Blyth, 2000: An investigation of ice production mechanisms in small cumuliform clouds using a 3D model with explicit microphysics. Part II: Case study of New Mexico cumulus clouds. *J. Atmos. Sci.,* **57,** 3004–3020.

Paluch, I. R., 1979: The entrainment mechanism in Colorado cumuli. *J. Atmos. Sci.,* **36,** 2467–2478.

Phillips, V. T. J., A. M. Blyth, P. R. A. Brown, T. W. Choularton, and J. Latham, 2001: The glaciation of a cumulus cloud over New Mexico. *Quart. J. Roy. Meteor. Soc.,* **127,** 1513–1534.

——, T. W. Choularton, A. M. Blyth, and J. Latham, 2002: The influence of aerosol concentrations on the glaciation and precipitation of a cumulus cloud. *Quart. J. Roy. Meteor. Soc.,* **128,** 951–971.

——, and Coauthors, 2005: Anvil glaciation in a deep cumulus updraft over Florida simulated with an explicit microphysics model. I: The impact of various nucleation processes. *Quart. J. Roy. Meteor. Soc.,* **131,** 2019–2046.

——, L. J. Donner, and S. T. Garner, 2007: Nucleation processes in deep convection simulated by a cloud-system-resolving model with double-moment bulk microphysics. *J. Atmos. Sci.,* **64,** 738–761.

Pruppacher, H. R., and J. D. Klett, 1997: *Microphysics of Clouds and Precipitation*. 2nd ed. Kluwer, 954 pp.

Raymond, D. J., and A. M. Blyth, 1986: A stochastic mixing model for nonprecipitating cumulus clouds. *J. Atmos. Sci.,* **43,** 2708–2718.

Rutledge, S. A., and P. V. Hobbs, 1984: The mesoscale and microscale structure and organization of clouds and precipitation in midlatitude cyclones. XII: A diagnostic modeling study of precipitation development in narrow cold-frontal rainbands. *J. Atmos. Sci.,* **41,** 2949–2972.

Sassen, K., and G. C. Dodd, 1988: Homogeneous nucleation rate for highly supercooled cirrus cloud droplets. *J. Atmos. Sci.,* **45,** 1357–1369.

Simpson, J., R. F. Adler, and G. R. North, 1988: A proposed Tropical Rainfall Measuring Mission (TRMM) satellite. *Bull. Amer. Meteor. Soc.,* **69,** 278–295.

Smolarkiewicz, P. K., and W. W. Grabowski, 1990: The multidimensional positive advection transport algorithm: Nonoscillatory option. *J. Comput. Phys.,* **86,** 355–375.

Soong, S.-T., and Y. Ogura, 1980: Response of trade wind cumuli to large-scale processes. *J. Atmos. Sci.,* **37,** 2035–2050.

Starr, D., and S. Cox, 1985: Cirrus clouds. Part I: Cirrus cloud model. *J. Atmos. Sci.,* **42,** 2663–2681.

Tao, W.-K., and J. Simpson, 1993: The Goddard Cumulus Ensemble model. Part I: Model description. *Terr. Atmos. Oceanic Sci.,* **4,** 19–54.

——, S. Lang, J. Simpson, C.-H. Sui, B. Ferrier, and M.-D. Chou, 1996: Mechanisms of cloud–radiation interaction in the tropics and midlatitudes. *J. Atmos. Sci.,* **53,** 2624–2651.

——, and Coauthors, 2003: Microphysics, radiation and surface processes in the Goddard Cumulus Ensemble (GCE) model. *Meteor. Atmos. Phys.,* **82,** 97–137.

Taylor, G. R., and M. B. Baker, 1991: Entrainment and detrainment in cumulus clouds. *J. Atmos. Sci.,* **48,** 112–121.

Warner, J., 1970: The microstructure of cumulus cloud. Part III: The nature of the updraft. *J. Atmos. Sci.,* **27,** 682–688.

Wei, D., A. M. Blyth, and D. J. Raymond, 1998: Buoyancy of convective clouds in TOGA COARE. *J. Atmos. Sci.,* **55,** 3381–3391.

Xie, S., and Coauthors, 2005: Simulations of midlatitude frontal clouds by single-column and cloud-resolving models during the Atmospheric Radiation Measurement March 2000 cloud intensive operational period. *J. Geophys. Res.,* **110,** D15S03, doi:10.1029/2004JD005119.

——, T. Hume, C. Jakob, S. Klein, R. McCoy, and M. Zhang, 2010: Observed large-scale conditions and diabatic heating and drying profiles during TWP-ICE. *J. Climate,* **23,** 57–79.

Xu, K.-M., and Coauthors, 2005: Modeling springtime shallow frontal clouds with cloud-resolving and single-column models. *J. Geophys. Res.,* **110,** D15S04, doi:10.1029/2004JD005153.

Zeng, X., and Coauthors, 2007: Evaluating clouds in long-term cloud-resolving model simulations with observational data. *J. Atmos. Sci.,* **64,** 4153–4177.

——, W.-K. Tao, S. Lang, A. Y. Hou, M. Zhang, and J. Simpson, 2008: On the sensitivity of atmospheric ensembles to cloud microphysics in long-term cloud-resolving model simulations. *J. Meteor. Soc. Japan,* **86A,** 45–65.

——, and Coauthors, 2009a: A contribution by ice nuclei to global warming. *Quart. J. Roy. Meteor. Soc.,* **135,** 1614–1629.

——, and Coauthors, 2009b: An indirect effect of ice nuclei on atmospheric radiation. *J. Atmos. Sci.,* **66,** 41–61.

Zhang, M. H., and J. L. Lin, 1997: Constrained variational analysis of sounding data based on column-integrated budgets of mass, heat, moisture, and momentum: Approach and application to ARM measurements. *J. Atmos. Sci.,* **54,** 1503–1524.

——, ——, R. T. Cederwall, J. J. Yio, and S. C. Xie, 2001: Objective analysis of ARM IOP data: Method and sensitivity. *Mon. Wea. Rev.,* **129,** 295–311.

Zipser, E. J., 2003: Some view on ''hot towers'' after 50 years of tropical field programs and two years of TRMM data. *Cloud Systems, Hurricanes, and the Tropical Rainfall Measuring Mission (TRMM), Meteor. Monogr.,* No. 51, Amer. Meteor. Soc., 49–58.